Available online at www.sciencedirect.com

ScienceDirect

Current Opinion in Cell Biology

Spatial patterning of energy metabolism during tissue morphogenesis

Bezia Lemma[1] and Celeste M. Nelson[1,2]

Abstract

Biophysical signaling organizes forces to drive tissue morphogenesis, a process co-opted during disease progression. The systematic buildup of forces at the tissue scale is energetically demanding. Just as mechanical forces, gene expression, and concentrations of morphogens vary spatially across a developing tissue, there might similarly be spatial variations in energy consumption. Recent studies have started to uncover the connections between spatial patterns of mechanical forces and spatial patterns of energy metabolism. Here, we define and review the concept of energy metabolism during tissue morphogenesis. We highlight experiments showing spatial variations in energy metabolism across several model systems, categorized by morphogenetic motif, including convergent extension, branching, and migration. Finally, we discuss approaches to further enable quantitative measurements of energy production and consumption during morphogenesis.

Addresses

[1] Department of Chemical and Biological Engineering, Princeton University, Princeton, NJ 08544, USA

[2] Department of Molecular Biology, Princeton University, Princeton, NJ 08544, USA

Corresponding author: Nelson, Celeste M. (celesten@princeton.edu)

Current Opinion in Cell Biology 2023, **85**:102235

This review comes from a themed issue on **Cell Signalling (2023)**

Edited by **JoAnn Trejo** and **Giorgio Scita**

For a complete overview see the Issue and the Editorial

Available online xxx

https://doi.org/10.1016/j.ceb.2023.102235

Abbreviations

AMPK, AMP-activated protein kinase; FGF, fibroblast growth factor; FLIM, fluorescence lifetime imaging microscopy; FRET, Förster resonance energy transfer; LDHA, lactate dehydrogenase A; NPC, nephron progenitor cell; OCR, oxygen consumption rate; PFKFB, 6-phosphofructo-2-kinase/fructose-2,6-biphosphatase 3; PSM, presomitic mesoderm.

Introduction

In the embryo, patterns of gene expression combine with mechanical forces to generate tissue form [1–5]. From a biophysical perspective, development is driven by chemical energy [6,7]. In addition to gene expression and mechanical forces, energy is also a critical and understudied parameter of morphogenesis. Concentrated energy in the form of sugars or ATP gives rise to cellular activity and, thus, tissue morphology. Some cells use energy in distinct manners identifiable from their energy metabolism and thermal energy dissipation. For instance, the Warburg effect, in which cells specifically resort to aerobic glycolysis, is a well-known hallmark of certain cancers. There may be equivalent hallmarks in developing tissues, and localized changes in energy patterns may predict or help explain patterns of development.

Here we review research on energy and energy metabolism during tissue morphogenesis. We first summarize the concepts of energy and energy metabolism with an eye toward understanding how measurements of energy may inform the field of developmental biology. We then highlight recent research in several model systems that show patterning of energy metabolism during tissue morphogenesis. For simplicity, we discretize our analysis by morphogenetic motif, including convergent extension, branching, and migration. Finally, we suggest some complementary experimental approaches that could be used to quantify spatial patterns of energy metabolism during morphogenesis.

Patterns of energy and energy metabolism

Changing a tissue from one geometry, such as a flat sheet, into another, such as a tube, requires energy. Concentrated sources of energy, such as ATP, can fuel these changes in tissue morphology. Given the dynamics of the process, it is reasonable to hypothesize that the energy required for tissue morphogenesis might vary in space and time. For instance, energy might vary spatially along the axis of extension in a tissue undergoing convergent extension. In contrast, energy might be concentrated at branch sites in a tissue undergoing branching (Figure 1a). Spatial patterns of energy might also depend on the identity of the tissue in addition to the morphogenetic motif. As an epithelium branches, its surrounding mesenchyme might consume energy at a different rate, resulting in spatial patterns across the two tissue layers (Figure 1b).

Figure 1

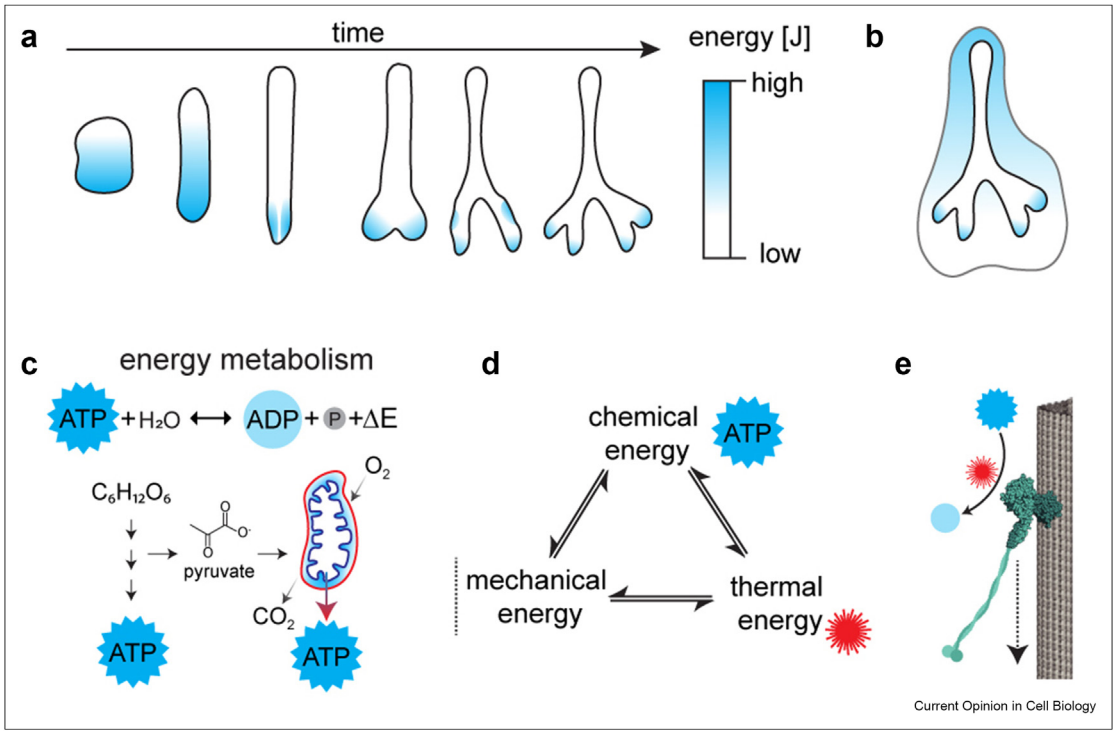

Patterns of energy metabolism during tissue morphogenesis. (**a**) Schematic of possible energy patterning in a tissue, first corresponding with convergent extension and then with branching morphogenesis. (**b**) Two layers of tissue with two different magnitudes and spatial patterns of energy. (**c**) Energy metabolism concentrates chemical energy in the form of ATP. Glycolysis uses glucose to produce ATP and provides pyruvate to fuel mitochondrial respiration, which produces ATP from energy stored in the mitochondrial intermembrane potential (indicated with red and blue). (**d**) Chemical, mechanical, and thermal energy all have units of joules [J] and are interlinked. (**e**) A motor protein walks, driven by chemical energy (indicated with the blue ATP/ADP symbol), and creates mechanical energy indicated by the dashed arrow. This process also releases thermal energy (indicated with the red thermal energy symbol).

Conversion of the concentrated chemical energy available in ATP to and from ADP is the central exchange of chemical energy in living systems. As concentrated energy is used, it becomes diluted, often transformed into thermal energy. Thus, the total energy *available* in a closed system to perform work can decrease. A fundamental aspect of biology is the influx of external concentrated energy to maintain or increase the total energy of the living system. At the molecular scale, intricate chemical reactions concentrate energy into ATP, a process termed energy metabolism (Figure 1c). Two major metabolic processes that take place during tissue morphogenesis are glycolysis and mitochondrial respiration. Measurements of the power [J/s] made accessible by energy metabolism can provide insights into which biological processes are being used to concentrate, convert, and dilute energy during morphogenesis.

Energy can take many forms; including chemical energy, mechanical energy, and thermal energy (Figure 1d), which can be measured in units of joules [J]. For instance, hydrolysis of ATP can convert its concentrated chemical energy into the mechanical energy of a molecular motor, which applies a force over a distance, while the remaining energy is dissipated into thermal energy [8] (Figure 1e). In turn, the mechanical energy of molecular motors might manifest as elastic energy or in the interfacial surface tension between cells [9,10].

The change in energy due to ATP hydrolysis, ΔE_{ATP-}, or ADP phosphorylation, ΔE_{ADP+}, has a chemical potential term, ΔE^0_{ATP-}, and an entropic term proportional to the logarithm of the ratio of the reactants to the products:

$$\Delta E_{ATP-} = -\Delta E_{ADP+} = E^0_{ATP-} + k_B T \ln\left(\frac{[ADP][P_i]}{[ATP][H_2O]}\right).$$

Where k_B is the Boltzmann constant, T is temperature, and the terms in square brackets indicate chemical concentrations. Cellular processes fueled by ATP hydrolysis are critical for tissue morphogenesis. Energy metabolism phosphorylates ADP with a power of $\partial E_{ADP+}/\partial t$ or $\partial_t E_{ADP+}$ [J/s]. The power produced by energy metabolism

may vary over space and time during tissue morphogenesis, which would result in spatiotemporal patterns of $\partial_t E_{ADP+}$.

Here, we summarize recent studies that have provided experimental evidence consistent with the hypothesis that energy metabolism associated with $\partial_t E_{ADP+}$ varies spatially during tissue morphogenesis. Conceptually, we have grouped these studies by morphogenetic motif for two main reasons. First, this conceptual grouping emphasizes the spatial component of measurements of energy metabolism. Second, this grouping takes advantage of an intuitively expected relationship between a given morphogenetic motif and the types of energy metabolism that might be spatially patterned during its occurrence. It is currently unknown whether different regions of a developing tissue consume chemical energy at different rates. Nonetheless, the studies highlighted here suggest that spatial patterns of energy metabolism might mirror patterns of change in tissue morphology.

Convergent extension

During convergent extension, a tissue lengthens along its major axis while simultaneously narrowing along its minor axis (Figure 2a). A prototypic example of this morphogenetic motif is elongation of the body axis. During elongation of the mouse embryonic body axis, an axial gradient of glycolytic activity has been observed in the presomitic mesoderm (PSM) (Figure 2b) [11]. Specifically, glucose uptake and glycolytic activity are highest in the posterior PSM, as revealed by imaging of the fluorescent glucose analog 2-(7-nitro-2,1,3-benzoxadiazol-4-yl)-D-glucosamine (2-NBDG) and *in situ* hybridization analysis of glycolytic enzymes. In contrast, fragments of anterior PSM have higher oxygen

Figure 2

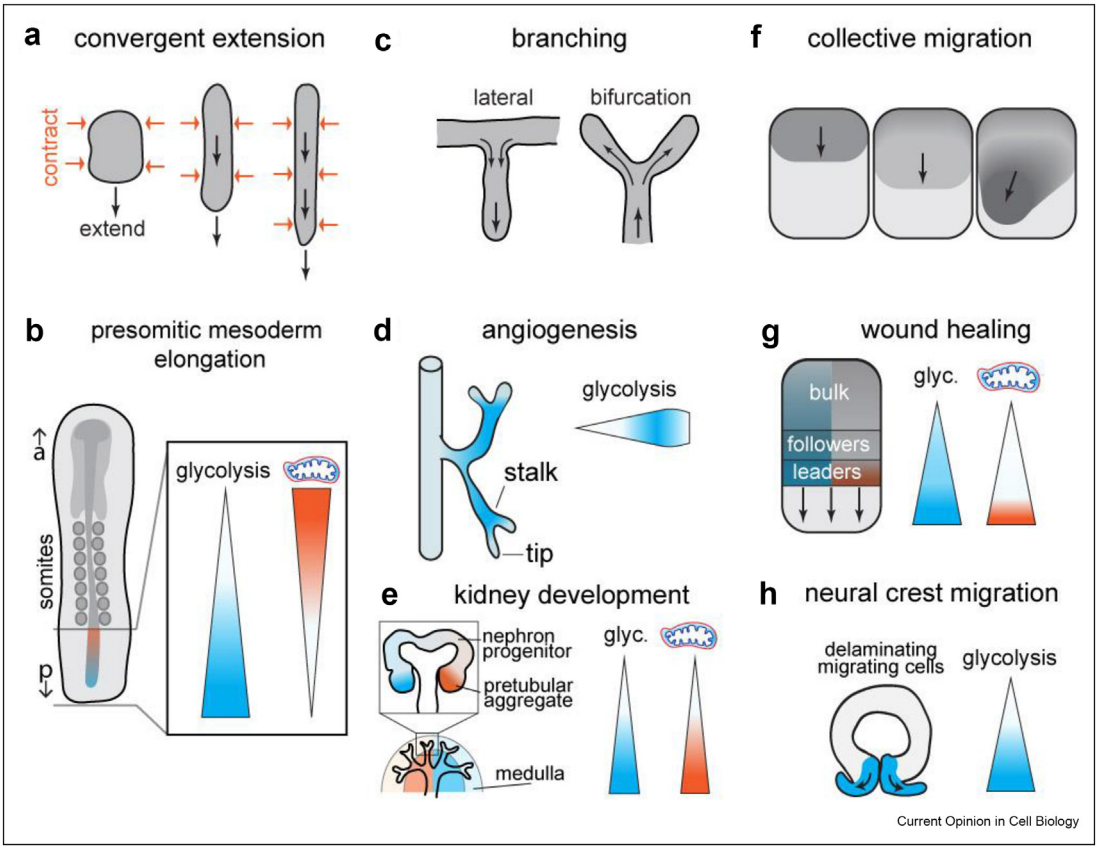

Gradients in energy metabolism, categorized by morphogenetic motif. (**a**) During convergent extension, tissue elongates in one direction and narrows in the perpendicular direction. (**b**) Convergent extension of the PSM in mouse and chicken embryos is accompanied by an increase in glycolysis towards the posterior (p↓), and an increase in OCR (indicated by the mitochondrion) in the anterior (a↑) end. (**c**) Tissues can arborize via lateral branching, the growth of new branches off a main stem, and bifurcations, the splitting of a main branch into two parts. (**d**) During angiogenesis, endothelial cells have increased glycolysis in the stalks and decreased glycolysis at the tips. (**e**) Gene-set enrichment analysis suggests higher glycolytic and mitochondrial ATP synthesis (indicated by the mitochondrion) during kidney development in the inner medullary region and in pretubular aggregates compared to nephron progenitor cells. (**f**) During collective migration, cells move together in a directed manner. (**g**) Wounded 2D monolayers display glycolytic activity that increases towards the motile follower and leader cells. Mitochondrial membrane potential (indicated by the mitochondrion) is observed at the leading edge of the migrating population. (**h**) During neural crest migration in chicken embryos, the population of delaminating migrating cells shows markedly increased glucose uptake and increased density of the glycolytic enzyme LDHA.

consumption rates (OCR) than fragments of posterior PSM. Consistently, mRNA expression screens revealed that more glycolytic genes are expressed at higher levels in the posterior undifferentiated PSM than in the anterior PSM. Levels of glycolysis were evaluated spatially by dissecting and culturing anterior and posterior PSM fragments separately in U−13C-glucose and then running these fragments through liquid chromatography-tandem mass spectrometry (LC-MS/MS). The levels of pyruvate, a product of glycolysis, were imaged via a Förster resonance energy transfer (FRET)-based sensor and found to decrease toward the anterior PSM as well. It is tempting to relate the increase in glycolytic activity at the posterior PSM to a local change in the rate of proliferation, as in the Warburg effect [12]. However, the authors noted that the rates of proliferation were spatially uniform within the PSM, which suggests that this spatial pattern of energy metabolism might instead correlate with mechanical forces that directly drive convergent extension.

The tail-bud region of the chicken embryo displays a similar posterior-to-anterior gradient in glycolysis during early phases of elongation [13]. As in mice, glucose uptake and glycolytic activity were assessed by imaging 2-NBDG and *in situ* hybridization analysis of glycolytic enzymes. In the tail bud, spatial gradients of transcription of glycolytic enzymes, downstream of fibroblast growth factor (FGF) signaling, were found to establish spatial gradients in glycolysis. In turn, glycolysis promoted elongation of the body axis of the embryo by increasing motility of cells in the PSM and coordinating signaling through Wnt and FGF.

Collectively, these studies revealed that spatial gradients in energy metabolism, specifically glycolysis, are present along the axis of elongating tissue in early mouse and chicken embryos. Body-axis elongation in zebrafish is accompanied by a continuous transition of cell motion from fluid-like in the mesodermal progenitor zone to solid-like behavior in the presomitic mesoderm [14]. It is possible that distinct metabolic processes correspond to distinct mechanical states or phases of cellular motion. Additional work is needed to link these spatial patterns of energy metabolism directly to chemical energy, which would provide a basis for understanding how chemical energy drives the physical dynamics of cellular activity during early elongation of the body axis.

Branching morphogenesis

In a branching system, new axes of tissue form at an angle relative to the axes of its parental branches. Branching modes include Y-shaped bifurcations, in which the parental axis splits into two daughter axes, and T-shaped lateral branches, in which a single branch emerges at an angle from the side of the parental branch (Figure 2c). Branch points are therefore spatially distinct from the parental tissue. Examples of branching tissues include the vasculature [15,16], the airways of the lungs, the collecting ducts of the kidneys [17], barbs of bird feathers [18], ray branching of fish fins [19], and the nervous system [20].

During angiogenesis, in which nascent blood vessels branch from existing vasculature, endothelial cells branch laterally to expand the vascular network. These angiogenic endothelial cells rely on glycolysis to produce ATP [21]. The glycolytic activator 6-phosphofructo-2-kinase/fructose-2,6-biphosphatase 3 (PFKFB3) regulates actin remodeling during angiogenesis, and the loss of PFKFB3 expression impairs vascular branching [22]. In culture, endothelial cells at the tip of a branch are less glycolytic than non-tip cells [23] (Figure 2d). Glycolysis was found to be necessary for the differentiation of tip cells, as revealed by siRNA-mediated knockdown of glycolytic enzymes PFKFB3 or lactate dehydrogenase A (LDHA) and the mitochondrial enzyme pyruvate dehydrogenase E1 subunit alpha 1 (PDHA1), both in culture and in the chick chorioallantoic membrane [24]. Oxidative phosphorylation by mitochondria may also be spatially patterned during angiogenesis: blood vessels incubated in a spatial gradient of oxygen significantly increase their rate of branching as compared to those incubated in spatially uniform levels of oxygen [25]. These findings suggest a spatial pattern of energy metabolism along the branches of nascent blood vessels, which may influence angiogenic sprouting.

The kidney is composed of an outer cortex and an inner medulla, populated by pyramidal structures that house the nephrons. As discrete filtering units of the kidney, the nephrons are connected to the ureter by a stochastically branched network of tightly packed collecting ducts [26]. Gene-set enrichment analysis suggests higher levels of mitochondrial ATP synthesis and usage in the medullary region compared to the outer cortex or renal pelvis (Figure 2e) [27]. Specifically, S-shaped body medial and proximal precursor cells and early proximal tubule and pre-tubular aggregate cells express high levels of genes associated with oxidative phosphorylation and glycolysis compared to nephron progenitor cells (NPCs). Furthermore, S-shaped body proximal precursor cells located in the inner medulla express higher levels of mitochondrial genes than proximal tubule cells. These spatial patterns of mitochondrial gene expression may be related to the energy requirements of kidney development or homeostasis.

The mammalian lung consists of a repeatedly branching series of epithelial tubes. This branching pattern starts with the trachea, which bifurcates into the two primary bronchi. From these primary bronchi, secondary and tertiary bronchi emerge using lateral branching and bifurcations. Surrounding and sculpting these branch

points is a layer of smooth muscle, which differentiates from the surrounding mesenchyme [28]. Single-cell RNA sequencing revealed that as the mesenchyme differentiates into smooth muscle, genes associated with proliferative metabolism are downregulated [29]. This change in metabolic profile suggests a shift in energy metabolism that mirrors the shift in differentiated function.

Sensory neurons grow with a branched geometry and then prune certain branches. Geometrically this is still a branched tissue, though dynamically it is distinct from other systems described here. Dendrite pruning in Drosophila sensory neurons requires AMP-activated protein kinase (AMPK), which regulates pyruvate usage related to mitochondrial energy metabolism. The loss of AMPK, as visualized using a FRET-based sensor, leads to defects in pruning factor translation [30]. This finding suggests that dendrite pruning may display distinct patterns of energy metabolism, particularly mitochondrial energy metabolism.

Collective migration

Tissues can change shape when their cells move collectively (Figure 2f). This collective migration can result in convergent extension, but it can also result in tissue expansion or contraction. Cell migration is energy-intensive: the cytoskeletal dynamics that drive migration account for nearly half of the ATP hydrolysis of a migrating cell [31,32].

A well-studied example of collective migration is wound healing, in which cells migrate toward an open wound in a manner guided by chemical and physical signals. Given the energetic costs of cell migration, one might expect significant spatial changes in energy metabolism during wound healing [33]. In monolayers of MDCKII epithelial cells, wounding results in three distinct populations: those migrating at the leading edge adjacent to the wound, those following just behind the leading edge, and those in bulk (Figure 2g) [34]. Glucose uptake, as measured by imaging 2-NBDG, increases throughout the monolayer in response to wounding, particularly in the cells at the leading edge. As measured by imaging tetramethylrhodamine ethyl ester perchlorate (TMRE), mitochondrial membrane potential also increases in the cells at the leading edge. In contrast, the cytoplasmic redox ratio NAD^+/NADH, as measured using the Peredox bioprobe, increases in the cells in bulk but not in those at the leading edge. These findings suggest that different regions of the migrating population exhibit spatially patterned metabolic adaptations during wound healing, potentially supporting the high energy demands of collective migration and wound closure.

An example of collective migration during embryonic development is the migration of neural crest cells from the neural tube. Immunostaining for the glycolytic enzyme LDHA in the chicken embryo shows a clear spatial population of migrating neural crest cells (Figure 2h) [35]. Consistently, transgenic chicken embryos expressing a fluorescent reporter of cytoplasmic glucose levels show a striking local increase in cranial neural crest cells. Additionally, the NAD^+/NADH ratio increases in this region, and 2-NBDG accumulates within neural crest cells. These results imply that migrating neural crest cells have higher rates of glycolysis than non-migrating cells.

Conclusions

The studies described above suggest spatial patterning of energy metabolism might be prevalent during tissue morphogenesis. During body-axis elongation in mouse and chicken embryos, a posterior-to-anterior gradient in glycolytic activity correlates with mechanical forces and cellular motion. During angiogenesis, the branching of endothelial cells depends on glycolysis, suggesting a patterning of energy metabolism related to both energy needs and signaling. During development of the kidney, the medullary region has higher levels of mitochondrial ATP synthesis and usage than the outer cortex. During development of the lung, proliferative metabolism is downregulated as the pulmonary mesenchyme differentiates into smooth muscle, which sculpts the shape of the adjacent epithelium. Dendrite pruning in Drosophila sensory neurons involves AMPK, and, thus, mitochondrial energy metabolism, suggesting distinct patterns of energy metabolism during this morphogenetic process. During wound healing, cells at the leading edge of the wound show increased glucose uptake and mitochondrial membrane potential. Finally, during early avian development, migrating neural crest cells show higher rates of glycolysis than non-migrating cells, potentially facilitating the energy-intensive process of collective migration.

These spatial observations are of energy metabolism-related proteins and cannot be directly quantified in terms of energy [J] or power [J/s]. Quantifying energy concentration and dilution in terms of ATP turnover would allow experiments to be validated against each other to produce a finer understanding of the energetics of morphogenesis. Measurements of the rates of oxygen consumption and extracellular acidification can be used to determine ATP production from respiration and glycolysis. Combined with measurements of ATP/ADP ratios, this information can be used to quantify the global chemical energy of ATP phosphorylation, $\partial_t E_{ADP+}$. Additionally, calorimetry can be used to measure thermal energy production over time.

Obtaining spatial resolution will require new techniques and fluorescent reporters. Significant progress has been made in studying the energy metabolism of single cells,

which could be applied to studying spatial patterns of energy metabolism during tissue development. Promising ATP concentration reporters and ATP/ADP ratio reporters have recently been reported, such as ATP-Red1 and Perceval [36–40]. Spatial patterns in the rate of oxygen consumption have been modeled based on fluorescence-lifetime imaging microscopy (FLIM) measurements of mitochondrial NADH levels [34,41,42]. pH reporters can provide information on the rate of glycolysis. A ratiometric FLIM-based sensor can also be used to give concentrations of glucose *in vivo* [43]. Furthermore, as pyruvate is a product of glycolysis, changes in pyruvate concentration can serve as a proxy for the rate of glycolytic ATP production [44]. At a larger scale, proton resonance frequency thermometry might provide time-resolved macroscopic or mesoscopic measurements of tissue temperature [45]. As we create tools to image and quantify chemical and thermal energy, we can link these energies to the mechanical energy that is deforming the tissue and thereby understand the fundamental energetic landscape of tissue morphogenesis.

Declaration of competing interest

The authors declare that they have no known competing financial interests or personal relationships that could have appeared to influence the work reported in this paper.

Data availability

No data was used for the research described in the article.

Acknowledgements

The authors are grateful to members of the Tissue Morphodynamics Group for helpful discussion. Work from the authors' group was supported by grants from the NIH (HD111539, HL164861, HD099030) and the NSF (2134935). B.L. was supported in part by the NSF Postdoctoral Research Fellowships Program in Biology (2305831).

References

Papers of particular interest, published within the period of review, have been highlighted as:

* of special interest

1. Collinet C, Lecuit T: **Programmed and self-organized flow of information during morphogenesis**. *Nat Rev Mol Cell Biol* 2021, **22**:245–265.

2. Muncie JM, Ayad NME, Lakins JN, Xue X, Fu J, Weaver VM: **Mechanical tension promotes formation of gastrulation-like nodes and patterns mesoderm specification in human embryonic stem cells**. *Dev Cell* 2020, **55**:679–694.

3. Cohen R, Amir-Zilberstein L, Hersch M, Woland S, Loza O, Taiber S, Matsuzaki F, Bergmann S, Avraham KB, Sprinzak D: **Mechanical forces drive ordered patterning of hair cells in the mammalian inner ear**. *Nat Commun* 2020, **11**:5137.

4. Subramanian A, Kanzaki LF, Schilling TF: **Mechanical force regulates Sox9 expression at the developing enthesis**. *Development* 2023, **150**, dev201141.

5. Trinh D-C, Alonso-Serra J, Asaoka M, Colin L, Cortes M, Malivert A, Takatani S, Zhao F, Traas J, Trehin C: **How mechanical forces shape plant organs**. *Curr Biol* 2021, **31**: R143–R159.

6. Yang X, Heinemann M, Howard J, Huber G, Iyer-Biswas S, Treut GL, Lynch M, Montooth KL, Needleman DJ, Pigolotti S, *et al.*: **Physical bioenergetics: energy fluxes, budgets, and constraints in cells**. *Proc Natl Acad Sci USA* 2021, **118**, e2026786118.

7. Ghosh S, Körte A, Serafini G, Yadav V, Rodenfels J: **Developmental energetics: energy expenditure, budgets and metabolism during animal embryogenesis**. In *Seminars in cell & developmental biology*. Elsevier; 2023:83–93.

8. Gilbert SP, Webb MR, Brune M, Johnson KA: **Pathway of processive ATP hydrolysis by kinesin**. *Nature* 1995, **373**: 671–676.

9. Maître J-L, Heisenberg C-P: **The role of adhesion energy in controlling cell–cell contacts**. *Curr Opin Cell Biol* 2011, **23**: 508–514.

10. Noll N, Mani M, Heemskerk I, Streichan SJ, Shraiman BI: **Active tension network model suggests an exotic mechanical state realized in epithelial tissues**. *Nat Phys* 2017, **13**:1221–1226.

11. Bulusu V, Prior N, Snaebjornsson MT, Kuehne A, Sonnen KF, Kress J, Stein F, Schultz C, Sauer U, Aulehla A: **Spatiotemporal analysis of a glycolytic activity gradient linked to mouse embryo mesoderm development**. *Dev Cell* 2017, **40**: 331–341.e334.

12. Koppenol WH, Bounds PL, Dang CV: **Otto Warburg's contributions to current concepts of cancer metabolism**. *Nat Rev Cancer* 2011, **11**:325–337.

13. Oginuma M, Moncuquet P, Xiong F, Karoly E, Chal J, Guevorkian K, Pourquié O: **A gradient of glycolytic activity coordinates FGF and Wnt signaling during elongation of the body Axis in amniote embryos**. *Dev Cell* 2017, **40**: 342–353.e310.

14. Mongera A, Rowghanian P, Gustafson HJ, Shelton E, Kealhofer DA, Carn EK, Serwane F, Lucio AA, Giammona J, Campàs O: **A fluid-to-solid jamming transition underlies vertebrate body axis elongation**. *Nature* 2018, **561**:401–405.

15. Guidolin D, Tamma R, Tortorella C, Annese T, Ruggieri S, Marzullo A, Ribatti D: **Morphometric analysis of the branching of the vascular tree in the chick embryo area vasculosa**. *Microvasc Res* 2020, **128**, 103935.

16. Dieterich LC, Tacconi C, Menzi F, Proulx ST, Kapaklikaya K, Hamada M, Takahashi S, Detmar M: **Lymphatic MAFB regulates vascular patterning during developmental and pathological lymphangiogenesis**. *Angiogenesis* 2020, **23**:411–423.

17. Goodwin K, Nelson CM: **Branching morphogenesis**. *Development* 2020, **147**:dev184499.

18. Chang W-L, Wu H, Chiu Y-K, Wang S, Jiang T-X, Luo Z-L, Lin Y-C, Li A, Hsu J-T, Huang H-L, *et al.*: **The making of a flight feather: bio-architectural principles and adaptation**. *Cell* 2019, **179**:1409–1423.

19. Braunstein JA, Robbins AE, Stewart S, Stankunas K: **Basal epidermis collective migration and local Sonic hedgehog signaling promote skeletal branching morphogenesis in zebrafish fins**. *Dev Biol* 2021, **477**:177–190.

20. Liao M, Liang X, Howard J: **The narrowing of dendrite branches across nodes follows a well-defined scaling law**. *Proc Natl Acad Sci USA* 2021, **118**, e2022395118.

21. Du W, Ren L, Hamblin MH, Fan Y: **Endothelial cell glucose metabolism and angiogenesis**. *Biomedicines* 2021, **9**:147.

22. De Bock K, Georgiadou M, Schoors S, Kuchnio A, Wong Brian W, Cantelmo Anna R, Quaegebeur A, Ghesquière B, Cauwenberghs S, Eelen G, *et al.*: **Role of PFKFB3-driven glycolysis in vessel sprouting**. *Cell* 2013, **154**:651–663.

23. * Yetkin-Arik B, Vogels IMC, Neyazi N, Vv Duinen, Houtkooper RH, CJFv Noorden, Klaassen I, Schlingemann RO: **Endothelial tip cells in vitro are less glycolytic and have a more flexible response to metabolic stress than non-tip cells**. *Sci Rep* 2019, **9**, 10414.

During angiogenesis, glycolysis is significantly lower in endothelial tip cells than in non-tip cells. Additionally, blocking mitochondrial respiration inhibits proliferation of non-tip cells.

24. Yetkin-Arik B, Vogels IMC, Nowak-Sliwinska P, Weiss A, Houtkooper RH, Noorden CJFV, Klaassen I, Schlingemann RO: **The role of glycolysis and mitochondrial respiration in the formation and functioning of endothelial tip cells during angiogenesis**. *Sci Rep* 2019, **9**, 12608.

25. Tran KA, Baldwin-Leclair A, DeOre BJ, Antisell M, Galie PA: **Oxygen gradients dictate angiogenesis but not barrier-genesis in a 3D brain microvascular model**. *J Cell Physiol* 2022, **237**:3872–3882.

26. Puelles VG, Combes AN, Bertram JF: **Clearly imaging and quantifying the kidney in 3D**. *Kidney Int* 2021, **100**: 780–786.

27. Wu H, Liu F, Shangguan Y, Yang Y, Shi W, Hu W, Zeng Z, Hu N, Zhang X, Hocher B, *et al.*: **Integrating spatial transcriptomics with single-cell transcriptomics reveals a spatiotemporal gene landscape of the human developing kidney**. *Cell Biosci* 2022, **12**:80.

28. Goodwin K, Lemma B, Zhang P, Boukind A, Nelson CM: **Plasticity in airway smooth muscle differentiation during mouse lung development**. *Dev Cell* 2023, **58**:338–347.

29. Goodwin K, Jaslove JM, Tao H, Zhu M, Hopyan S, Nelson CM: **Patterning the embryonic pulmonary mesenchyme**. *iScience* 2022, **25**, 103838.

30. * Marzano M, Herzmann S, Elsbroek L, Sanal N, Tarbashevich K, Raz E, Krahn MP, Rumpf S: **AMPK adapts metabolism to developmental energy requirement during dendrite pruning in Drosophila**. *Cell Rep* 2021, **37**, 110024.

AMPK is required to regulate dendrite pruning, an energetically costly and spatially intricate developmental transition. Neurons lacking AMPK rely more on glycolysis than oxidative phosphorylation for ATP production. AMPK locally promotes oxidative phosphorylation and pyruvate usage, and loss of AMPK or mitochondrial deficiency causes defects in pruning factor translation.

31. Bernstein BW, Bamburg JR: **Actin-ATP hydrolysis is a major energy drain for neurons**. *J Neuro* 2003, **23**. 1.2–6.

32. Daniel JL, Molish IR, Robkin L, Holmsen H: **Nucleotide exchange between cytosolic ATP and F-actin-bound ADP may be a major energy-utilizing process in unstimulated platelets**. *Eur J Biochem* 1986, **156**:677–683.

33. Wang X-H, Yang F, Pan J-B, Kang B, Xu J-J, Chen H-Y: **Quantitative imaging of pN intercellular force and energetic costs during collective cell migration in epithelial wound healing**. *Anal Chem* 2020, **92**:16180–16187.

34. * DeCamp SJ, Tsuda VMK, Ferruzzi J, Koehler SA, Giblin JT, Roblyer D, Zaman MH, Weiss ST, Kölöç A, Marzio MD, *et al.*: **Epithelial layer unjamming shifts energy metabolism toward glycolysis**. *Sci Rep* 2020, **10**, 18302.

In a two-dimensional wound healing assay, an advancing layer of leader and follower epithelial cells becomes more fluid-like than jammed bulk cells. These advancing populations shift energy metabolism towards glycolysis and mitochondrial activity.

35. * Bhattacharya D, Azambuja AP, Simoes-Costa M: **Metabolic reprogramming promotes neural crest migration via yap/tead signaling**. *Dev Cell* 2020, **53**:199–211.

Migration of neural crest cells is correlated with a relative increase in glycolysis compared to surrounding tissue. This increase in glycolytic flux promotes Yap/Tead signaling, which drives an epithelial-to-mesenchymal transition.

36. Wang L, Yuan L, Zeng X, Peng J, Ni Y, Er JC, Xu W, Agrawalla BK, Su D, Kim B, Chang YT: **A multisite-binding switchable fluorescent probe for monitoring mitochondrial ATP level fluctuation in live cells**. *Angew Chem Int Ed* 2016, **55**: 1773–1776.

37. Berg J, Hung YP, Yellen G: **A genetically encoded fluorescent reporter of ATP:ADP ratio**. *Nat Methods* 2009, **6**:161–166.

38. Sun W, Liu G, Tong M, Wang H, Liu S: **A mitochondria-targeting fluorescent sensor for on–off–on response to Cu 2+ and ATP in cells and zebrafish**. *Analyst* 2021, **146**:1892–1896.

39. Huang B, Liang B, Zhang R, Xing D: **Molecule fluorescent probes for adenosine triphosphate imaging in cancer cells and in vivo**. *Coord Chem Rev* 2022, **452**, 214302.

40. Lobas MA, Tao R, Nagai J, Kronschläger MT, Borden PM, Marvin JS, Looger LL, Khakh BS: **A genetically encoded single-wavelength sensor for imaging cytosolic and cell surface ATP**. *Nat Commun* 2019, **10**:711.

41. Yang X, Ha G, Needleman DJ: **A coarse-grained NADH redox model enables inference of subcellular metabolic fluxes from fluorescence lifetime imaging**. *eLife* 2021, **10**, e73808.

42. Blacker TS, Mann ZF, Gale JE, Ziegler M, Bain AJ, Szabadkai G, Duchen MR: **Separating NADH and NADPH fluorescence in live cells and tissues using FLIM**. *Nat Commun* 2014, **5**:3936.

43. Díaz-García CM, Lahmann C, Martínez-François JR, Li B, Koveal D, Nathwani N, Rahman M, Keller JP, Marvin JS, Looger LL, Yellen G: **Quantitative in vivo imaging of neuronal glucose concentrations with a genetically encoded fluorescence lifetime sensor**. *J Neuro Res* 2019, **97**:946–960.

44. Arunachalam E, Ireland W, Yang X, Needleman D: *Dissecting flux balances to measure energetic costs in cell biology: techniques and challenges*. 2022. arXiv , eprint = 220500969.

45. Odéen H, Parker DL: **Magnetic resonance thermometry and its biological applications – physical principles and practical considerations**. *Progr Nucl Magn Reson Spectrosc* 2019, **110**: 34–61.